Quantum Mechanical Investigation of Thiourea Adsorption on Ag(111) Considering Electric Field and Solvent Effects

E. M. Patrito,*,† F. P. Cometto,‡ and P. Paredes-Olivera‡

Instituto de Investigaciones en Fisicoquímica de Córdoba (INFIQC), Facultad de Ciencias Químicas, Universidad Nacional de Córdoba, Ciudad Universitaria, 5000 Córdoba, Argentina

Received: April 20, 2004; In Final Form: July 27, 2004

The adsorption of different thiourea species was investigated on the 111 surface of silver considering electric field and solvent effects with the objective of (a) elucidating the nature of the adsorbed species, mainly in an electrochemical environment, and (b) understanding the energetics and mechanisms of the surface reactions, particularly the oxidative adsorption of thiourea. We first considered the adsorption in vacuum of molecular species such as thiourea (TU), canonical thiourea, and formamidine disulfide as well as the adsorption of the canonical thiourea radical resulting from the cleavage of the S−H bond. The molecular adsorption of TU in vacuum has the highest binding energy (−33.2 kcal/mol) when the molecular plane is parallel to the surface. However, the strongest surface bond was observed for the canonical thiourea radical (−42.2 kcal/mol) whose nature is the same as that of the methanethiol radical. Externally applied electric fields perpendicular to the surface have an important effect on the orientation and surface bonding of thiourea, leading to an upright configuration of the molecule and to a strengthening of the sulfur−surface bond. Solvent effects were first considered to investigate the equilibria of thiourea in solution with the purpose of elucidating the nature of the predominant species which, in turn, constitutes the initial adsorbate on the surface. In neutral and basic pHs, the thiourea molecule is the predominant species, whereas in acidic electrolytes, the thiouronium ion readily forms. The microsolvation of thiourea with up to 16 water molecules was investigated to determine the structure of the hydration shell and the interaction energy between TU and water molecules. Water molecules form a compact cage around thiourea characterized by linked tetramer and pentamer structures. The NH_2 groups form hydrogen bonds with water molecules, whereas the sulfur atom is poorly hydrated. The implications of the structure of water around thiourea on the adsorption geometry of the molecule are discussed. The oxidative adsorption mechanism of thiourea resulting in chemisorbed canonical thiourea was investigated considering charge-transfer processes, solvent effects, and the presence of a counterion.

Introduction

Thiourea (TU) is widely used in the electrodeposition of metals such as copper and silver from aqueous solutions. The reagent is introduced into electrolytes to influence deposit morphology, such as smoothness and grain size.[1−3] The underpotential deposition of copper on platinum[4] and gold[5] is also significantly influenced by the presence of TU in solution. The adsorption of TU on different metal electrode surfaces also has a catalytic effect on the hydrogen-evolution reaction,[6] and its electrochemical response has been investigated on active metals such as Pt.[6−8] TU is also a corrosion inhibitor of copper and iron in acidic media.[9−13] Radiometric methods were employed to measure surface concentrations of ^{14}C-labeled thiourea on silicon,[14] silver,[15] and copper[16] surfaces. On the metallic electrodes, the adsorption of thiourea was found to be reversible.[15−16] On the silver surface,[15] the values of TU surface concentration are compatible with a structure in which the molecules adsorb perpendicular to the surface.

Surface-enhanced Raman spectroscopy has been extensively used to study the adsorption of thiourea and several isostructural compounds such as thioamide, thiohydrazide, and thiocarbohydrazide on silver and copper surfaces.[17−30] In most cases, it was found that these molecules are bonded via the sulfur atom to Ag and Cu surfaces. The substantial downshift in the frequencies of vibrational modes having a predominant contribution from C═S stretching suggested considerable electronic interactions between these molecules and metal surfaces. Some authors have also reported that thiourea may undergo orientational changes from an essentially perpendicular geometry depending on the TU concentration and the type of electrolyte anion.[17,19,22] The reorientation of thiourea from perpendicular to parallel to the surface was also reported on silver on the positive side of the adsorption maximum in a radiochemical study.[15]

The surface chemistry of thiourea on silver is very rich under electrochemical conditions. A radiotracer study showed that the adsorption takes place in the entire range of potentials accessible to surface studies on silver electrodes.[15] The thermodynamic information for this system indicated that the interaction of TU with silver falls into the chemisorption category rather than the physisorption category.[15] The nature of the surface chemical bond was recently addressed in a combined electrochemical and XPS study[31] in which it was found that TU oxidatively adsorbs as thioureate, the canonical form of thiourea with a cleaved S−H bond. The nature of the adsorbed species also depends on the electrode potential. Under mild oxidation conditions, thioureate

* Corresponding author. Tel: 54-351-4334169/54-351-4334180. Fax: 54-351-4334188. E-mail: martin@fcq.unc.edu.ar.
† Departamento de Fisicoquímica .
‡ Unidad de Matemática y Física.

10.1021/jp048278r CCC: $27.50
Published on Web 09/11/2004

molecules oxidize originating formamidine disulfide (FDS).[31] The importance of the substrate−adsorbate interaction was confirmed by STM because of the correlation of the observed structures with those of sulfur on the highly symmetric Ag(111) and Au(111).[32]

On the theoretical side, the adsorption of TU on metal surfaces has not been investigated yet. Ab initio calculations have been reported for TU in the gas phase in studies of thiourea protonation,[33] in the formation of chains and ribbons,[34] and in spectroscopic calculations.[35]

In the present paper, we investigated the interaction of different TU species with the Ag(111) surface under conditions that simulate the environment of the electrochemical double layer. The objective was to understand the energetics and the nature of the adsorbed species as well as the surface reactions in which they are involved. We considered the adsorption of the molecular species thiourea, $(NH_2)_2CS$ (Figure 1), canonical thiourea, $(NH)(NH_2)CSH$ (Figure 1), and formamidine disulfide, $((NH)(NH_2)SC)_2$ (Figure 2) as well as the adsorption of the canonical thiourea radical, $(NH)(NH_2)CS^{\bullet}$, resulting from the cleavage of the S−H bond. As a starting point, the adsorption studies were performed under vacuum conditions. However, for a molecule with a high dipole moment, such as thiourea, and with the capability of forming hydrogen bonds, solvent effects cannot be neglected. Solvent effects were first considered for thiourea in solution to investigate the equilibria with hydronium and hydroxide ions with the purpose of identifying the predominant species in the solution. The microsolvation of thiourea was then addressed with up to 16 water molecules, and the implications of the structure of the solvation shell on the adsorption geometry of thiourea on Ag(111) were discussed. The simulation of the electrical double-layer environment was first taken into account by applying externally homogeneous electric fields perpendicular to the surface. To improve the double-layer modeling, we then investigated the adsorption of a partially hydrated TU molecule on a positively charged surface together with a fluoride anion to ensure electroneutrality. In this environment, the mechanism of oxidative adsorption of TU was studied in detail. The model was able to describe the proton transfer to the solution as well as the electron transfer toward the metal.

This paper is organized as follows. We first consider the structure of the different species in vacuum and then the adsorption of these species on Ag(111) also under vacuum conditions. As an initial step in the modeling of the electrochemical double layer, the surface bonding of thiourea is investigated in the presence of external electric fields perpendicular to the surface. Solvent effects are considered for thiourea in the form of a dielectric medium as well as explicitly with up to 16 water molecules. Finally, the mechanism of thiourea−thioureate conversion is addressed both in vacuum and in an electrochemical environment.

Theoretical Methods and Surface Modeling

The interaction of thiourea with water molecules and hydronium and hydroxide ions was investigated using density functional theory (DFT) at the B3LYP level. The split valence basis set 6-31G, augmented with polarization and diffuse functions, 6-31+G(d,p), was employed. It is widely accepted that for a proper description of anionic systems diffuse functions are necessary but for a proper description of hydrogen bonds the use of diffuse functions is also of utmost importance. The addition of one set of diffuse functions centered on nonhydrogen atoms is, by far, more important than the addition of the second set centered on hydrogen atoms. If diffuse functions are omitted, then higher basis set superposition errors (BSSE) and shorter hydrogen-bond lengths are obtained in comparison with those of more complete basis sets. Thus, the 6-31+G(d,p) basis provides an adequate description of electron distributions within the individual molecules and in the intermolecular regions. For these DFT calculations, we used the B3LYP functional because hybrid functionals provide an accurate description for systems with hydrogen bonds with an accuracy comparable to that of MP2 calculations.[34,36] The Gaussian 03 program[37] was used for these calculations.

The interaction of closed-shell molecules with the metal surface was investigated at the second-order perturbation level of theory (MP2). DFT was not used in these calculations because it underestimates binding energies because of its well-known deficiency in accounting for the London dispersion forces.[38] The binding energies calculated at the MP2 level were obtained using a 28-metal-atom cluster model of the Ag(111) surface with three layers (12, 10, and 6 atoms in each layer, Figure 3, inset). The atoms in the first metal layer were described using 11-electron atoms, and the remainder of the atomic electron density was replaced by relativistic effective core potentials (RECP) of the Huzinaga type.[39−41] The basis set employed for the 11-electron silver atoms is a (7s1p2d/3s1p2d) RECP basis set. The contraction coefficients were fit to reproduce the atomic orbitals and orbital energies as obtained from relativistic Hartree−Fock calculations in which the Darwin and mass−velocity corrections were taken into account. The metal atoms in the second and third layers had only one electron in the valence shell. For the sulfur, carbon, nitrogen, and hydrogen atoms, we employed a double-ζ plus polarization basis set.[42] The metal cluster was built using the bulk metal distance of 2.884 Å for silver.[43] The calculations were done using the electronic structure program TANGO-95.[44]

The interaction of the canonical thiourea radical and the methanethiol radical with the metal surface was investigated at the DFT level using the Amsterdam density functional program (ADF).[45] The Ag(111) surface was modeled using a cluster with 25 metal atoms distributed in two layers (16 atoms in the first layer and 9 in the second layer, see Figure 10). The same type of metal atom was employed for both layers to investigate the relaxation of the atoms in the primary chemisorption site induced by the adsorbate. The ADF program was used because of its excellent convergence properties in systems containing many metal atoms. ADF represents molecular orbitals as linear combinations of atomic Slater-type orbitals. Kohn−Sham one-electron equations are solved using the Vosko−Wilk−Nusair (VWN) functional[46] to obtain the local potential. To correct the overbinding inherent in the local density approximation (LDA), we used a gradient-corrected exchange energy functional. Gradient corrections for the exchange (Becke functional[47]) and correlation (Perdew functional[48]) energy terms were self-consistently included. The binding energies of the canonical TU radical and the methanethiol radical that were calculated with the BP86 functional[47,48] were also compared with the binding energies obtained using the BLYP[47,49] and PW91[50] functionals. We observed very good agreement between the different functionals giving binding energies that did not differ by more than 2 kcal/mol. As we point out in the chemisorption section, these binding energies are in good agreement with the MP2 calculations.

To enhance computational efficiency, we kept the innermost atomic shells of the silver atoms frozen (up to and including the 4f orbitals) because these core electrons do not contribute

significantly to the chemical bonding. Relativistic effects were taken into account using the zero-order regular approximation (ZORA).[51] A triple-ζ STO basis set with one set of polarization functions was utilized for the adsorbate atoms as provided in the package (basis set IV, comparable to 6-311G*). For the metal atoms, we used a double-ζ STO basis set with one set of polarization functions (basis set II).

The binding energies were calculated by subtracting the total energy of the bare substrate and the bare adsorbate from the substrate−adsorbate composite energy

$$BE = E_{\text{adsorbate-cluster}} - E_{\text{adsorbate}} - E_{\text{cluster}} \qquad (1)$$

Negative values of the binding energies indicate a stabilization of the substrate−adsorbate system with respect to the bare adsorbate and bare metal cluster. In the case of alkanethiol adsorption on metal surfaces, considerable charge transfer takes place, leading to the formation of thiolate anions on the surface.[52] Therefore, larger metal clusters are required for adsorbates with important charge transfer to/from the surface. In our previous work on alkanethiol adsorption on Cu(111),[53] we showed that for metal clusters of more than 25 atoms converged binding energies with cluster size are obtained.

The hydration of thiourea and canonical thiourea was investigated using the polarizable continuum model (PCM).[54] The united atom topological model was used to generate the cavity that defines the solute−solvent boundary.

Vibrational frequency calculations were performed for all systems except for the largest ones containing many metal atoms. Vibrational frequencies provide control so that the stationary points localized are correct, with no imaginary frequencies for minima and one imaginary frequency for transition states. They are also used to estimate the zero-point vibrational effects on energy.

Results and Discussion

Thiourea, Canonical Thiourea, and Formamidine Disulfide in Vacuum. In this section, we consider the energetics and structure of the adsorbates in vacuum. Figure 1 shows the structure of TU and several conformers of canonical TU. The equilibrium structure of TU in vacuum has C_2 symmetry with pyramidal NH_2 groups. However, previous DFT studies have shown that the energy difference between TU with C_2, C_s, and C_{2v} symmetry is very small, less than 1 kcal/mol at the DFT level.[34] Planar TU (C_{2v} symmetry) is the transition state for the inversion process of TU with C_2 symmetry.[35] Figure 1 shows the equilibrium structures of four conformers of canonical TU. Frequency calculations confirm that they correspond to a true minimum. The total energies as well as the thermal corrections are shown in Table 1 for the different structures optimized at the B3LYP/6-31+G(d,p) and B3LYP/6-311+G(2df,2p) levels. ΔG values at 298 K show that the different structures of canonical TU are between 11 and 15 kcal/mol less stable than those of TU. The two most stable structures have the NH group with the hydrogen atom pointing away from the other NH_2 group (structures 1 and 2 in Figure 1). The calculations performed with the medium and large basis sets confirm that structure 2 is the most stable conformer of canonical TU, although for both basis sets, the energy difference between conformer 1 and 2 is only 0.2 kcal/mol. Table 2 contains the geometric data of the molecules calculated at the B3LYP/6-31+G(d,p) and B3LYP/6-311+G(2df,2p) levels. The main differences between TU and canonical TU are observed in the SC bond length, which is larger for canonical TU, and in the CN bond length, which for

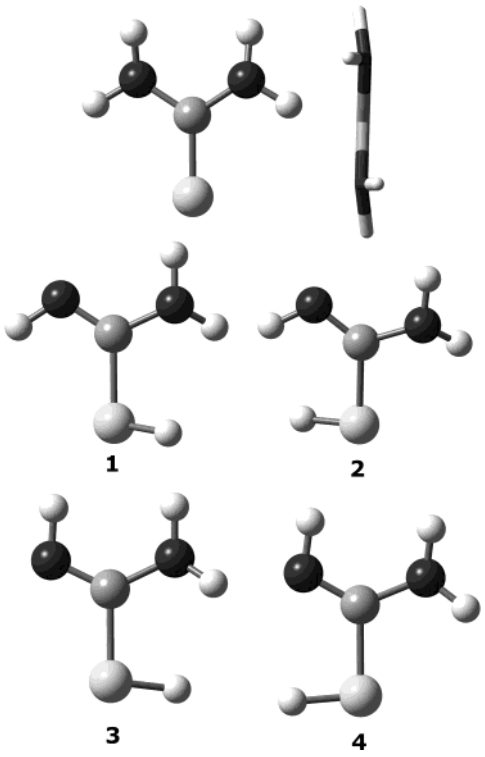

Figure 1. Equilibrium structures of thiourea (front and side views showing pyramidal NH_2 groups) and four conformers of canonical thiourea. B3LYP/6-311+(2df,2p) calculations.

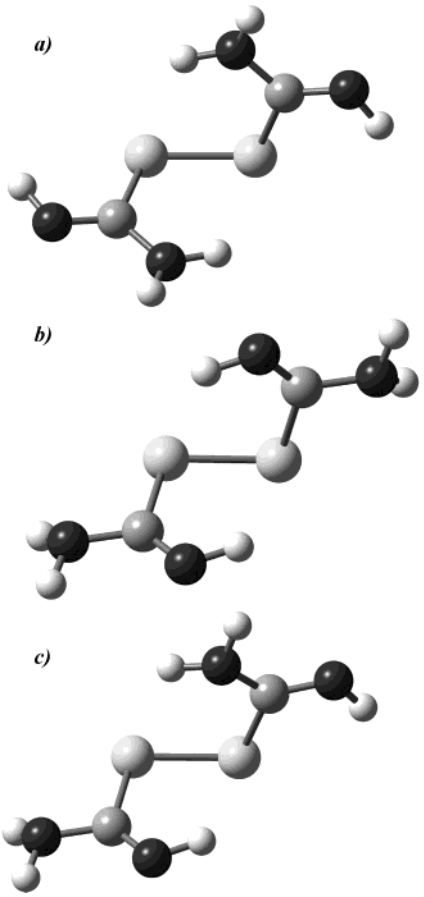

Figure 2. Different conformers of formamidine disulfide. B3LYP/6-311+(2df,2p) calculation.

TU is intermediate between a single and a double bond. The SCN angles for TU and canonical TU are around 120°, revealing

TABLE 1: Total Electronic Energy, Free Energy, and Dipole Moments of Thiourea and Canonical Thiourea Conformers Calculated with Medium and Large Basis Sets

	6-31+G(d,p)				6-311+G(2df,2p)			
	total energy /au	G /au	ΔG_{298} kcal/mol	μ/D	total energy /au	G /au	ΔG_{298} kcal/mol	μ/D
TU	−548.240479	−548.206213	0.00	5.16	−548.316187	−548.282002	0.00	5.01
1	−548.215764	−548.185622	12.9	2.36	−548.293496	−548.263495	11.6	2.38
2	−548.216229	−548.185995	12.7	1.56	−548.293744	−548.263832	11.4	1.52
3	−548.213179	−548.183706	14.1	2.88	−548.290731	−548.261435	12.9	2.77
4	−548.209600	−548.180012	16.4	4.27	−548.288263	−548.258639	14.7	4.01

TABLE 2: Geometrical Parameters (Bond Lengths in Å, Bond Angles and Dihedral Angles in deg) of Thiourea and the Canonical Thiourea Conformers Shown in Figure 1

	TU	1	2	3	4
S−C	1.674/1.667	1.820/1.807	1.824/1.814	1.799/1.793	1.799/1.791
C−N1	1.367/1.361	1.274/1.267	1.274/1.266	1.276/1.268	1.275/1.267
C−N2	1.367/1.361	1.381/1.376	1.377/1.373	1.385/1.380	1.391/1.385
N1−H		1.017/1.014	1.016/1.012	1.023/1.019	1.022/1.018
N2−H1	1.011/1.007	1.014/1.010	1.012/1.008	1.011/1.007	1.013/1.009
N2−H2	1.009/1.005	1.010/1.006	1.010/1.005	1.011/1.006	1.011/1.007
S−H		1.349/1.344	1.346/1.341	1.345/1.340	1.349/1.344
S−C−N1	122.7/122.6	124.0/123.4	128.0/127.8	119.8/120.1	116.6/116.4
S−C−N2	122.7/122.6	114.4/114.9	110.3/110.4	111.7/111.6	115.0/115.4
N1−C−N2	114.6/114.8	121.7/121.8	121.6/121.7	128.4/128.2	128.4/128.2
H−S−C		96.6/97.2	95.1/95.2	93.6/93.6	96.5/97.0
S−C−N1−N2	180.0/180.0	179.2/179.7	175.4/176.0	−176.4/−176.9	−178.3/−1785
S−C−N2−H1	158.7/160.2	173.4/171.9	177.4/176.2	−169.1/−167.8	−171.7/−169.7
S−C−N2−H2	8.4/8.2	36.5/33.6	36.1/33.9	−26.2/−24.1	−33.7/−30.9
S−C−N1−H		7.9/7.5	4.5/4.1	179.4/179.6	174.3/175.2
N2−C−S−H		34.6/28.4	−156.5/−159.8	175.5/177.0	−23.9/−18.7

TABLE 3: Total Electronic and Free Energy of the Three Formamidine Disulfide Conformers Shown in Figure 2

FDS	total energy /au	G /au	ΔG_{298} /kcal/mol
a	−1095.235660	−1095.173269	0.00
b	−1095.236111	−1095.171886	0.87
c	−1095.235966	−1095.172779	0.31

the sp^2 hybridization of the carbon atom. The SH bond lengths of the different canonical TU structures are in the range of 1.340−1.344 Å (for 6-311+G(2df,2p) basis), whereas for the prototype methanethiol molecule, the SH bond length is 1.342 Å, indicating that the molecular environment does not influence the SH bond length.

Figure 2 shows the three lowest energy conformers of FDS. They are obtained from canonical TU structure 1, and they have facing NH_2, NH, and NH_2−NH groups. The energetic and geometrical parameters of the conformers are listed in Figures 3 and 4. The energy difference between the different conformers is less than 1 kcal/mol. The structure in Figure 2a (with facing NH_2 groups) has the smallest CSSC dihedral angle and the longest S−S bond length, whereas the opposite trend is observed for the structure in Figure 2b (with facing NH groups). With the energetics in Tables 1 and 3, we can evaluate the energy change for the reaction

$$2 \text{ canonical TU} \rightarrow \text{FDS} + H_2 \qquad (2)$$

Taking into account the zero-point vibrational energies, this reaction is endothermic by 5.7 kcal/mol (B3LYP/6-311+G-(2df,2p)). In summary, the most stable species in vacuum is thiourea followed by canonical TU (Figure 1, structure 2), which is 11.4 kcal/mol higher in energy. In turn, the products of reaction 2 leading to the formation of FDS are 5.7 kcal/mol higher in energy than canonical TU.

Interaction with the Ag(111) Surface in Vacuum. *A. Physisorption.* In this section, we consider the interactions of

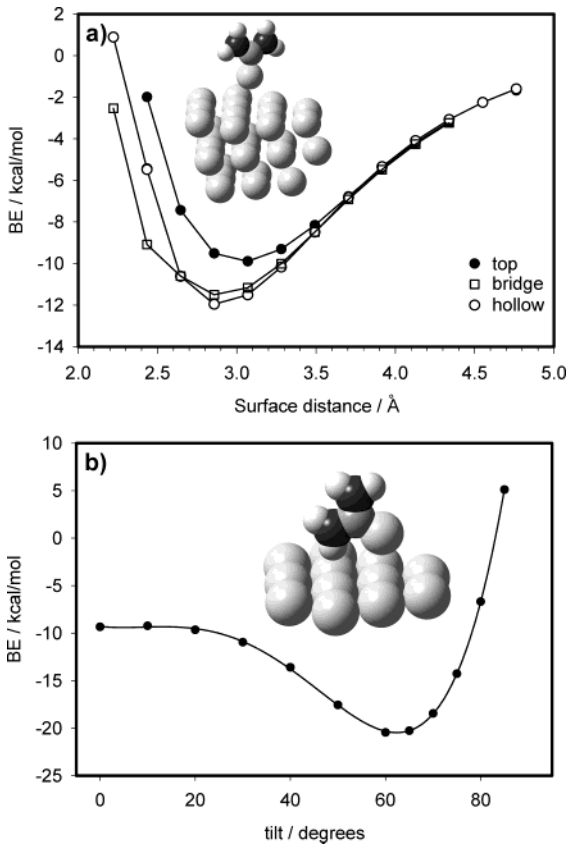

Figure 3. Potential energy curves for (a) upright thiourea adsorption via the sulfur atom and (b) tilted adsorption (molecular plane perpendicular to the surface) via the sulfur atom and the NH_2 group. The surface normal and the line along the SC bond define the tilt angle. The inset in a shows the adsorbate and the metal cluster. The inset in b shows the tilted adsorbate and only the first layer of metal atoms. MP2/DZP(adsorbate)+DZ-Huzinaga ECP (metal) calculation.[42,44]

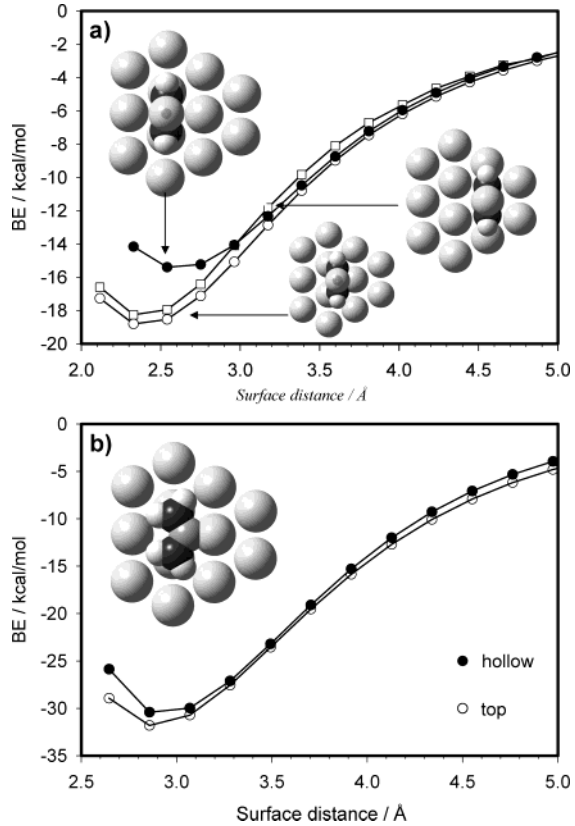

Figure 4. Potential energy curves for (a) upright adsorption via the NH_2 groups and (b) flat adsorption. MP2/DZP(adsorbate)+DZ-Huzinaga ECP (metal) calculation.[42,44] The inset shows only the first layer of metal atoms.

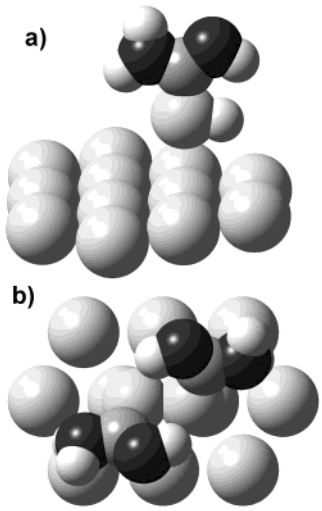

Figure 5. Molecular geometries considered for (a) canonical thiourea and (b) formamidine disulfide adsorbed on the on-top sites of Ag(111). MP2/DZP(adsorbate)+DZ-Huzinaga ECP (metal) calculations.[42,44] The inset shows only the first layer of metal atoms.

TU, canonical TU, and FDS with different surface sites of Ag(111) and for different coordinations of the adsorbates with the surface. The potential energy curves for TU that is adsorbed perpendicular to the surface via the sulfur atom are shown in Figure 3 for adsorption on hollow, bridge, and on-top sites. The potential energy curves are sensitive to the surface site only for sulfur−surface distances smaller than 3.5 Å. As Table 5 shows, the binding energies are between −9.9 and −12 kcal/mol with the hollow site being 2.1 kcal/mol more stable than the on-top site. For the bridge and hollow sites, the equilibrium sulfur−surface distance is 2.86 Å, whereas for the on-top site, it is larger, 3.1 Å. When the TU molecule is tilted (Figure 3b), the interaction of the NH_2 group with the surface increases the binding energy. The equilibrium position is found for a tilt of 60° of the SC bond with respect to the surface normal. The binding energy for this bicoordinated TU is −20.5 kcal/mol. The potential energy curve in Figure 3b corresponds to a TU molecule adsorbed with the sulfur atom on an on-top site. At the equilibrium tilt angle of 60°, the NH_2 group is located on a bridge site.

TABLE 4: Geometrical Parameters (Bond Lengths in Å, Bond Angles and Dihedral Angles in deg) of Formamidine Disulfide Conformers Shown in Figure 2

	a	b	c
S−S	2.089	2.057	2.072
S−C	1.841	1.858	1.839
S−S−C	107.8	102.6	107.6
C−S−S−C	−88.5	−94.9	−93.3

TABLE 5: Equilibrium Binding Energies of Thiourea, Canonical Thiourea, and Formamidine Disulfide Adsorbed in Various Configurations on the Different Surface Sites of Ag(111)

adsorbate	coordination	surface site	BE /kcal/mol
TU	upright, via S	top	−9.9
TU	upright, via S	hollow	−12.0
TU	upright, via S	bridge	−11.5
TU	upright, via NH_2	top	−18.3
TU	upright, via NH_2	hollow	−18.5
TU	upright, via NH_2	bridge	−15.4
TU	tilted, via S and NH_2	S on top	−20.5
TU	flat	S on top	−33.2
canonical TU	upright, via SH	SH on top	−7.7
canonical TU	tilted via SH and NH_2	SH on top	−17.5
FDS	via S atoms	S on top	−17.0

The potential energy curves for upright adsorption via the NH_2 groups and for flat adsorption are shown in Figure 4. Adsorption via the NH_2 groups yields binding energies that are higher than those yielded from adsorption via the sulfur atom (Figure 3a). The highest binding energies are obtained when the NH_2 groups are approximately located on bridge and hollow sites. The surface distance in Figure 4a corresponds to the perpendicular distance of the hydrogen atoms closer to the surface. When the TU molecule is flat on the surface, the highest binding energy is obtained. Two surface sites were investigated for flat adsorption: one has the S and NH_2 groups on an on-top position (inset of Figure 4b), and the other has these atoms on hollow sites. Figure 4b and Table 5 show that the corrugation of the potential energy surface is very small, indicating that the barrier for surface diffusion of flat TU is small. For the on-top adsorption, a binding energy of 33.2 kcal/mol was obtained at the equilibrium position, which has the molecular plane 2.86 Å above the surface.

In summary, the data in Table 5 show that each molecular group coordinated to the surface contributes around −10 kcal/mol to the binding energy: adsorption via the sulfur atom has an average BE of −11.1 kcal/mol; adsorption via both NH_2 groups or via the S and one NH_2 group yields an average BE of −19.1, and flat adsorption (involving both NH_2 and the sulfur atom) has a BE of −33.2 kcal/mol. Therefore, under low-coverage conditions, adsorption with the molecular plane parallel to the surface is the most stable configuration in vacuum, whereas adsorption via the sulfur atom has the lowest binding energy. These results seem to contradict the spectroscopic data of TU adsorption in solution,[17−30] which indicate that TU

TABLE 6: Comparison of Canonical Thiourea Radical and Methanethiol Radical Surface Bonding on Different Surface Sites of Ag(111)

	canonical TU radical			methanethiol radical		
surface site	BE kcal/mol	surface distance/Å	charge transfer/au	BE kcal/mol	surface distance/Å	charge transfer/au
fcc	−35.8 (−42.2)	2.15	0.21	−39.6 (−44.1)	2.13	0.17
hcp	−33.5 (−41.1)	2.12	0.23	−38.1 (−47.6)	2.17	0.18
bridge	−32.5	2.20	0.22	−36.0	2.08	0.15
top	−24.9	2.60	0.24	−26.3	2.56	0.16

adsorbs via the sulfur atom. Clearly, the solvent and the electric field at the interphase must play an important role in determining the adsorption geometry of thiourea. These issues will be discussed in forthcoming sections.

In the calculations shown in Figures 3 and 4, we first used the TU geometry optimized in vacuum. Then, the SC bond was relaxed in the equilibrium positions of TU and was adsorbed with an upright (Figure 3a) and with a flat configuration (Figure 4b). We found that the SC bond length increases only by 0.02 Å, indicating that the interaction with the surface has virtually no influence on the bond strength. This small relaxation has no effect on the computed binding energies using the vacuum geometry of TU.

We also considered the energetics of canonical TU and FDS adsorbed with the sulfur atoms on on-top sites (Figure 5). The binding energy of canonical TU in an upright configuration (Figure 5a) is −7.7 kcal/mol and increases up to −17.5 kcal/mol for an equilibrium tilt of 60°. These binding energies are only a few kilocalories/mole less negative than those for TU in comparable coordinations. However, taking into account that the most stable canonical TU conformer is 11.4 kcal/mol less stable than TU, the surface reaction

$$SC(NH_2)_{2(surf)} \rightarrow HSC(NH_2)(NH)_{(surf)} \qquad (3)$$

is endothermic by +15.7 kcal/mol. This indicates that it is unlikely that canonical TU may molecularly adsorb as shown in Figure 5a. Figure 5b shows an FDS molecule adsorbed with the sulfur atoms approximately on on-top sites. This molecule is produced during the oxidation of TU.[11,12] We obtained a binding energy of −17 kcal/mol for the on top coordination, shown in Figure 5b. As we will show in the next section, FDS is unstable on the Ag(111) surface and decomposes into two canonical TU radicals.

B. Chemisorption. To complete the picture of possible adsorbed species derived from TU, in this section, we investigate the adsorption of the canonical TU radical, $(NH)(NH_2)CS^{\bullet}$, which is obtained by the cleavage of the SH bond of canonical TU (Figure 1). In a recent XPS investigation of TU on Ag(111), it was observed that the energy window of the S 2p peak is the same as that for alkanethiolates, suggesting that the canonical TU radical is the species adsorbed from aqueous solutions.[31] Therefore, we compare here the surface bonding of this radical with that of the prototype methanethiol radical, $CH_3S^{\bullet}$, to elucidate the extent to which the bonding of the TU radical resembles that of the methanethiol radical. Table 6 contains the binding energies, equilibrium sulfur−surface distances, and adsorbate charge that were calculated on different surface sites. The binding energies were first calculated with the S−C bond perpendicular to the surface and without considering the relaxation of the adsorbate and the surface. Table 6 shows that for the canonical TU and methanethiol radicals comparable binding energies are obtained. The same trend is observed in both cases: the on-top site is the least stable, whereas the other sites have comparable binding energies. The sulfur−surface distance and the charge transferred from the surface to the adsorbate also reveal that the bonding of canonical TU is similar to that of methanethiol. For both species, there is a charge transfer of about 0.2 electrons toward the adsorbate, indicating that the nature of the adsorbed species is ionic. For the fcc and hcp hollow sites, we also investigated the surface bonding considering the relaxation of the adsorbate and the three metal atoms in the primary chemisorption site. The binding energies including relaxation effects increase in magnitude up to 9 kcal/mol (Table 6, numbers in parentheses). The binding energies of canonical TU on the fcc and hcp hollow sites differ only by 1 kcal/mol, whereas in the case of methanethiol, the hcp hollow site is more stable.

The adsorption of the TU radical produces an outward and upward displacement of the three atoms of the hollow site. The interatomic distance of the metal atoms increases from the bulk value of 2.89 to 3.01 and 3.03 Å for the fcc and hcp sites, respectively, and the displacement above the surface is 0.10 and 0.16 Å, respectively. In the case of methanethiol, the interatomic distance increases to 3.01 (fcc) and 3.00 Å (hcp), and the atoms move above the surface 0.15 (fcc) and 0.19 Å (hcp). Therefore, both adsorbates produce a comparable relaxation of the substrate.

The C−S bond length of the adsorbed TU radical considerably increases in comparison to that of the C−S bond of TU in vacuum. The calculated value in vacuum with ADF is 1.668 Å (in very good agreement with the B3LYP/6-311+G(2df,2p) value of 1.667 Å reported in Table 2), whereas the C−S bond length of the adsorbed canonical TU radical is 1.843 (fcc) and 1.853 Å (hcp). The increase of nearly 0.2 Å in the C−S bond length upon adsorption explains the substantial downshift in the frequencies of vibrational modes having a predominant contribution from C−S stretching reported in the literature.[17−30] However, as pointed out in the previous section, for molecularly adsorbed TU either with an upright (Figure 3a) or a flat configuration (Figure 4b), the S−C bond length increased only 0.02 Å, indicating that the interaction with the surface has virtually no influence on the bond strength. Therefore, we conclude that the considerable downshift of the C−S stretching modes is the consequence of chemical bonding of TU in its canonical form.

The binding energies of the radical species calculated in this section at the DFT level on the Ag(111) surface compare very well with previous calculations on Cu(111) performed at the MP2 level.[53] The binding energy of $SCH_3^{\bullet}$ is −39.6 kcal/mol on the fcc site of Ag(111) (Table 6, without surface relaxation) and −43 kcal/mol on the same site on Cu(111) (Figure 1, ref 53). We see that the DFT binding energy on silver is coherent with the MP2 value on copper: silver is less active than copper and has a smaller binding energy. However, the binding energies do not differ too much, and this is the case for chemisorbed molecular adsorbates on metal surfaces.[55]

With the binding energies calculated in this section, we can now evaluate the surface stability of FDS according to the following reaction

$$(NH)(NH_2)CS-SC(NH_2)(NH)_{(surf)} \rightarrow 2(NH)(NH_2)CS^{\bullet}_{(surf)} \quad (4)$$

The energy change of this reaction is given by

$$\Delta E = -BE_{FDS} + D_{S-S} + 2BE_{TU} \quad (5)$$

which results from the thermodynamic cycle in which FDS is desorbed ($-BE_{FDS}$), the S−S bond is broken (D_{S-S}), and two canonical TU radicals are adsorbed on the surface ($2BE_{TU}$). For D_{S-S}, we obtained a value of 50.0 kcal/mol at the B3LYP/6-311+G(2df,2p) level including zero-point energy corrections. With $BE_{FDS} = -17$ kcal/mol calculated in the previous section and $BE_{TU} = -42.2$ kcal/mol on the fcc hollow site (Table 6), we obtain $\Delta E = -17.4$ kcal/mol. Thus, the reaction is very exothermic, indicating that FDS will decompose into two canonical TU radicals on the surface. An analogous reaction has been observed on Au(111): the decomposition of dimethyl disulfide into two methanethiol radicals.[56] With the data in Table 1 of ref 56, we calculate $\Delta E = -13.7$ kcal/mol (dimethyl disulfide on top, $\Theta = 0.5$, and $CH_3S + CH_3S$ on a bridge site with $\Theta = 0.5$). Therefore, the dissociative adsorption of disulfides seems to be a general trend for the coinage metals. We note that dimethyl disulfide binding energies between −4.4 and −5.9 kcal/mol reported in ref 56 are underestimated as a consequence of the limitations of DFT in handling dispersion forces.[38] For example, for TU adsorbed via the S atom, we obtained a binding energy of −9.9 kcal/mol (on top site) at the MP2 level, whereas at the DFT level (with ADF basis sets), we obtained only −2 kcal/mol. This is the reason that the adsorption of closed-shell molecules was treated at the MP2 level in this work. Adsorption via a sulfur atom contributes around 10 kcal/mol to the binding energy. As another example, we can mention the binding energies of $HSCH_3$ and H_2S calculated by Sellers[57] at the MP2 level on Au(111): −12.7 and −9.4 kcal/mol, respectively. However, even if the binding energy of dimethyl disulfide on Au were as high as that of FDS on Ag (the binding energies of closed-shell molecules are similar on Au and Ag[55]), it would still dissociatively adsorb on Au.

Electric Field Effects. To model the environment of the electrochemical double layer, we consider in this section the adsorption of TU in the presence of external, uniform electric fields applied in a direction perpendicular to the surface. Electric fields in the range of ±0.01 au = ±5.2 10^7 V/cm were considered. A positive field polarizes the electron density of the bare cluster, leaving the surface layer with a depletion of electron density with respect to the zero-field situation; the reverse trend is observed for negative fields. The modeling of electrode polarization by applying external, uniform electric fields can be considered to be a first approximation in the study of electrode processes. In a later section, we consider a more realistic situation in which an inhomogeneous electric field is generated between an oxidized metal cluster and a counterion. The main objective of this section is to investigate the influence of the electric field of the double layer on the bonding of TU to the metal surface. The study of electric field effects on adsorbate properties such as binding energy and equilibrium adsorbate−surface distance is very useful because it permits us to discriminate the effective charge of the adsorbate. As expected, electric field effects are more pronounced for charged[58] adsorbates than for neutral adsorbates.[59]

For TU adsorbed on the Ag(111) surface, the electric field has an important effect on the surface bonding, and different physical process contribute to this effect. Figure 6 shows the variation of *BE* with electric field for TU adsorbed on the hollow site. At positive fields, the binding energy increases from −12.0 kcal/mol (zero field) to −41.0 kcal/mol at a field of +0.01 au. When negative fields are applied, the binding energy decreases, and at a field of −0.01, the interaction is repulsive by 6.4 kcal/mol. Figure 6b shows that the sulfur−surface distance decreases for the most positive fields. In the range of electric fields that were investigated, the surface distance varies by 0.3 Å, from 3.0 to 2.7 Å. The increase in the sulfur−surface distance together with the decrease in binding energy explains the fact that at sufficiently negative potentials TU desorbs.[14,15]

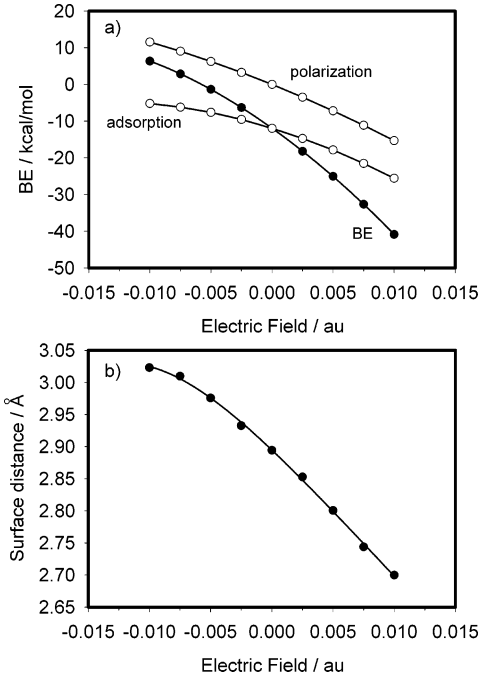

Figure 6. Electric field effects on the surface bonding of thiourea. (a) Polarization and adsorption contributions to the binding energy and (b) sulfur−surface distance. Homogeneous electric fields were applied in a direction perpendicular to the surface. MP2/DZP(adsorbate)+DZ-Huzinaga ECP (metal) calculations.[42,44]

To understand the different contributions to the binding energy, we have decomposed the overall adsorption process in the presence of electric fields

$$\text{TU in vacuum} + \text{metal cluster (electric field)} \rightarrow \text{adsorbed TU (electric field)} \quad (6)$$

into the following steps:

Polarization.

$$\text{TU in vacuum} \rightarrow \text{TU in vacuum (electric field)} \quad (7)$$

Adsorption.

$$\text{TU in vacuum (electric field)} \rightarrow \text{adsorbed TU (electric field)} \quad (8)$$

In step 7, an electric field is applied to a TU molecule in vacuum, and the energy change of this process is the polarization energy of TU. In step 8, both the adsorbate and the metal cluster representing the surface are subject to the same electric field, and they are brought together for the adsorption process to take place. The energy change of this step is the adsorption energy. We will refer to the energy change of the whole reaction, process 6, as the binding energy that is decomposed into polarization and adsorption energies.

The energies of the different processes are shown in Figure 6a. For the most positive field of 0.01 au, the polarization energy contributes −15.3 kcal/mol to the binding energy, and the adsorption energy contributes −25.6 kcal/mol. However, for a negative field of −0.01 au (opposed to the dipole moment of thiourea) the polarization contribution is +11.6 kcal/mol, and the adsorption contribution is only −5.2 kcal/mol, producing an overall repulsive $BE = +6.4$ kcal/mol. We attribute the strengthening of the surface bond at positive fields to the electrostatic interaction between the negatively charged sulfur atom (see charges in Figure 7) and the increasingly positive surface charge induced by the electric field. The increase in binding energy at positive fields is also accompanied by partial charge transfer from TU toward the metal surface. With a field of +0.01 au, the charge transfer toward the metal is 0.1 electrons. This partial charge transfer represents the initial state in the process of TU oxidation toward more oxidized products such as canonical thioureate and FDS.

The results of this section indicate that the electric field has an important effect on the binding energy and the adsorption geometry. Although in the absence of electric fields, the most stable adsorption geometry corresponds to a flat TU molecule on the surface (Table 5), in the presence of sufficiently positive electric fields, the upright configuration coordinated via the sulfur atom becomes the preferred adsorption geometry. For this configuration, the polarization of TU makes an important contribution to the binding energy because the dipole moment of TU is aligned with the electric field. Under negative electric fields, the most stable configuration corresponds to TU bound to the surface via both NH_2 groups because it has the TU dipole moment aligned with the field. However, this geometry has not been observed experimentally. We need to consider the microhydration of TU to explain why this geometry is unlikely in solution.

We also investigated electric field effects for the canonical TU radical. Whereas the binding energy of the radical is −35.8 kcal/mol on the fcc site (without considering the adsorbate and surface relaxation, Table 6) in vacuum, it increases to −42.4 kcal/mol in the presence of a field of +0.01 au. The surface distance decreases from 2.15 to 2.08 Å. Electric field effects are less important for the canonical TU radical than for TU. This is to be expected for two reasons: first, the radical is strongly chemically bound to the surface, and second, the dipole moment of the radical (2.0 D) is smaller than that of TU (5.0 D).

Solvent Effects. *Thiourea Equilibria in Acidic and Basic Solutions.* In this section, we investigate the chemistry of thiourea in solution considering the reaction with hydronium and hydroxide ions. We first represent the solvent as a dielectric and use the PCM model to calculate hydration free energies. The characterization of the acid−base equilibria in solution is important to the identification of the nature of the species that adsorb on the metal surface.

Figure 7 shows the equilibrium structures that were obtained after the reaction of TU with hydronium and hydroxide ions. The hydronium−TU complex in Figure 7a was optimized with the O−S distance constrained to a fixed value of 3.5 Å. At this O−S distance, the hydronium ion begins to decompose. The OH bond length of the hydrogen atom pointing toward the sulfur atom is 1.066 Å, whereas the other OH bond lengths are 0.979 Å. The geometry optimizations were repeated for different initial positions of the hydronium ion, but in the final structure, the ion is always located in front of the sulfur atom as shown in Figure 7a. Mulliken populations show that the sulfur atom of free TU bears an effective charge of −0.51 electrons, whereas the nitrogen atoms bear a charge of −0.24 electrons, explaining the preference of hydronium for the sulfur atom. In a study of protonated thiourea, it was found that protonation via the sulfur atom is 20 kcal/mol more stable than that via either of the nitrogen atoms.[33] In Figure 7a, the hydronium ion has an effective charge of +0.8 electrons, indicating that some partial discharge has occurred. When the O−S constraint is relaxed, a proton is transferred to the sulfur atom, giving rise to a thiouronium ion that has an effective charge of +0.96 (Figure 7b). A comparison of the Mulliken populations of thiouronium and thiourea shows that most of the positive charge of the cation is located along the CSH fragment.

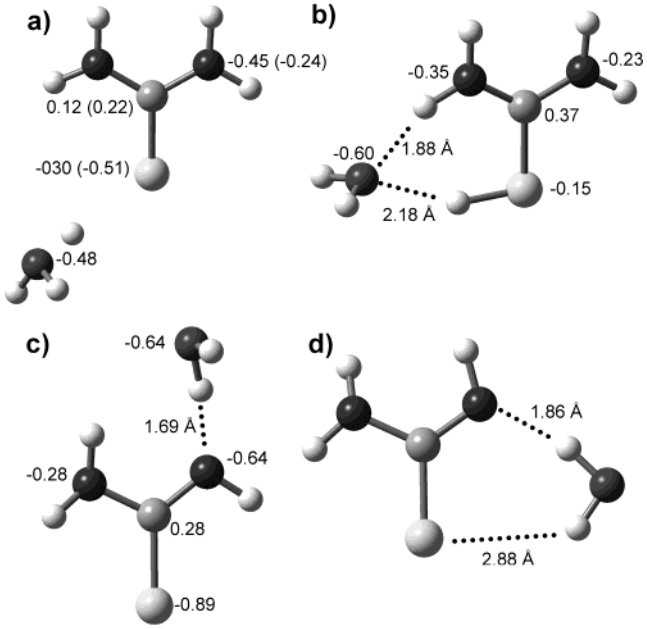

Figure 7. Reaction products of thiourea with hydronium and hydroxide ions. The numbers indicate Mulliken charges in atomic units and hydrogen bond lengths. (a) Equilibrium structure obtained by fixing the O−S distance at 3.4 Å. Numbers in parentheses correspond to Mulliken charges of free TU (N, C, and S atoms). (b) Hydrated thiouronium ion obtained after protonation of thiourea by hydronium. (c) and (d) Equilibrium structures of thioureate anions generated by the deprotonation of different hydrogens of thiourea. B3LYP/6-311+-(2df,2p) calculations.

The reaction of hydroxide with thiourea produces two different thioureate anions depending on which hydrogen atom of TU reacts with hydroxide. The structure in Figure 7c is 6.1 kcal/mol more stable than that in Figure 7d. The hydrogen bond between water and TU in Figure 7c is much shorter than that in Figure 7d. The effective charge of thioureate in Figure 7c is −0.97 electrons with the negative charge mainly located on the sulfur atom and on the nitrogen atom hydrogen bonded to water.

The structural parameters of thiouronium (TU^+) and thioureate (TU^-) in vacuum together with those of thiourea are collected in Table 7. The S−C bond length increases for TU^+ and TU^-. The C−N bond lengths for TU and TU^+ are intermediate between those of single and double bonds, whereas for TU^-, two different C−N bond lengths of 1.295 and 1.410 Å are obtained.

Table 8 contains the energetics in vacuum of all of the species involved in the reaction of TU with the hydronium or hydroxide ion.

$$SC(NH_2)_2 + H_3O^+ \rightarrow HSC(NH_2)^+ + H_2O \quad (9)$$

$$SC(NH_2)_2 + OH^- \rightarrow {}^-SC(NH)(NH_2) + H_2O \quad (10)$$

The free-energy change of these reactions in solution, ΔG_{sol}, can be evaluated according to the following thermodynamic cycle

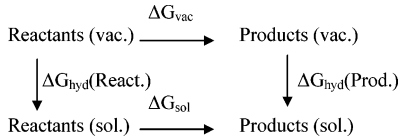

where ΔG_{vac} is the free energy in vacuum and ΔG_{sol} is the free energy for transferring a molecule in vacuum to a continuous medium characterized by a dielectric constant ϵ. Therefore, ΔG_{sol} can be computed from

$$\Delta G_{sol} = \Delta G_{vac} + \Delta G_{hyd}(prod) - \Delta G_{hyd}(react) \quad (11)$$

The free energy corresponding to a given reaction in vacuum, ΔG_{vac}, was computed according to

$$\Delta G_{vac} = \Delta E_{elect} + \Delta ZPE + \Delta E_T - T\Delta S \quad (12)$$

In eq 12, ΔE_{elect}, ΔZPE, ΔE_T, and ΔS are the differences in the electronic energy, zero-point energy, thermal energy, and entropy between the product(s) and reactant(s), respectively. The geometries of the reactant(s) and the product(s) were fully optimized at the B3LYP/6-31+G(d,p) and B3LYP/6-311+G-(2df,2p) levels of theory, and their vibrational frequencies were evaluated at the same level of theory. No imaginary frequencies were found in any of the molecules studied. The zero-point energy, thermal energy, and entropy corrections were evaluated at 298.15 K using standard statistical mechanical equations.[60]

With the data in Table 8, we calculated ΔE_{vac} and ΔG_{vac} as shown in Table 9. The reaction of TU with hydronium is more exothermic than that with the hydroxide anion. Table 9 also shows that basis set effects and thermal corrections are more important in the reaction with hydronium. To evaluate ΔG_{sol}, the hydration free energies of the different species are required (eq 11). They were calculated using the PCM model[54] and are listed in Table 10. It is well documented that the PCM model gives quite accurate values for species such as OH^-, H_3O^+, and H_2O as well as neutral and charged organic molecules.[54] Using these hydration energies, we obtained a negative free-energy change of -4.9 kcal/mol for the reaction of TU with hydronium, whereas the reaction with hydroxide anion gives a positive ΔG_{sol} of 3.6 kcal/mol. With these free-energy values and the corresponding p*K* values listed in Table 9, we conclude that in neutral and alkaline solutions the predominant species is thiourea, whereas in acidic solutions, the thiouronium cation will be readily formed.

In Table 1, we show that canonical TU is 11.4 kcal/mol less stable than TU in vacuum (B3LYP/6-311+G(2df,2p) level). When the solvent was taken into account, we obtained $\Delta G_{298} = 16.1$ kcal/mol at the same level of theory. Therefore, the energy difference in water between TU and canonical TU is greater than that in vacuum, indicating that canonical TU is less stable than TU. The reason for the lower stability in water becomes clear when we consider the dipole moments of both species listed in Table 1, 5.01 D for TU and 1.52 D for canonical TU. The much lower dipole moment of canonical TU implies a lower electrostatic contribution to the hydration energy in comparison with that of TU.

TABLE 7: Comparison of Geometrical Parameters of Thiouronium (TU^+) and Thioureate (TU^-) Ions with Those of Thiourea[a]

	TU	TU^+	TU^-
S−C	1.667	1.744	1.752
C−N1	1.361	1.323	1.295
C−N2	1.361	1.323	1.410
N1−H			1.014
N2−H1	1.007	1.010	1.011
N2−H2	1.005	1.007	1.006
S−H		1.344	
S−C−N1	122.6	122.5	128.8
S−C−N2	122.6	116.6	115.3
N1−C−N2	114.8	120.9	115.9
H−S−C		96.0	

[a] Bond lengths in Å, bond angles in deg.

TABLE 8: Total Electronic and Free Energies of All of the Species Involved in the Reaction of Thiourea with Hydronium and Hydroxide Ions

	6-31+G(d,p)		6-311+G(2df,2p)	
	total energy /au	G_{298} /au	total energy /au	G_{298} /au
TU	−548.240479	−548.206213	−548.316187	−548.282002
TU^+	−548.587568	−548.544397	−548.666384	−548.623480
TU^-	−547.677538	−547.655785	−547.750991	−547.729357
OH^-	−75.8034348	−75.811143	−75.8296874	−75.837362
H_3O^+	−76.7077678	−76.691578	−76.7344596	−76.718184
H_2O	−76.4340476	−76.430410	−76.4625638	−76.458854

Microsolvation of Thiourea. In this section, we address the structure of the hydration shell and the interaction energy between TU and the water molecules in connection to the adsorption process in an aqueous environment. The microsolvation of TU was investigated with up to 16 water molecules. In the building of each hydrated structure, the water molecules were added from different initial positions. For the less hydrated TU complexes, we observed different local structures. This is shown in Figure 8a and b for the monohydrated complex and in Figure 8c and d for the bihydrated complex. For complexes with more than two water molecules, we plotted only the lowest-energy structures in Figure 8e−i. Vibrational frequencies were computed for all of the structures to verify that they corresponded to true minima. The general feature observed in these optimizations was a competition between intrawater hydrogen bonding and water−TU hydrogen bonding. Thus, whereas in Figure 8e and f both hydrogens of the NH_2 group are involved in hydrogen bonding with water molecules, only one hydrogen of the NH_2 group remains hydrogen bonded to water when more water molecules are added. This is due to the energetically more favorable formation of water trimers (Figure 8h) and then tetramers and pentamers (Figure 8i) around the NH_2 groups. Although we cannot claim that we have scanned the full configuration space, we note that the structure of $TU-(H_2O)_{16}$ shown in Figure 8i was obtained from several geometry optimizations that started from different initial configurations. The reason for the stability of this structure is clear: water molecules cluster around TU, forming the stable tetramer and pentamer structures found in liquid water in agreement with molecular dynamics simulations.[61] Thus, we consider this structure to be quite representative of the first hydration shell of TU.

The water pentamers around TU in the $TU-(H_2O)_{16}$ structure (Figure 8i) have hydrogen-bond lengths in the range of 1.64−2.19 Å with an average bond length of 1.87 Å, indicating that for $TU-(H_2O)_{16}$ the water cage around TU is very compact. This can also be appreciated when comparing the O−O distance

TABLE 9: Energetics of the Reactions of Thiourea with Hydronium and Hydroxide in Vacuum and in Solution[a]

	ΔE_{vacuum}		ΔG_{vacuum}		ΔG_{sol}	pK
	6-31+G(d,p)	6-311+G(2df,2p)	6-31+G(d,p)	6-311+G(2df,2p)		
$H_3O^+ + TU \rightarrow TU^+ + H_2O$	−46.0	−49.1	−48.3	−51.6	−4.9	3.6
$OH^- + TU \rightarrow TU^- + H_2O$	−42.5	−42.5	−43.2	−43.2	3.6	−2.6

[a] Energies in kcal/mol.

TABLE 10: Hydration Free Energies of the Species Involved in the Reaction of Thiourea with Hydronium and Hydroxide Ions

	ΔG_{hyd} /kcal/mol
TU	−14.7
TU^+	−67.8
TU^-	−66.3
OH^-	−104.8
H_3O^+	−106.1
H_2O	−6.4

of an isolated water pentamer in vacuum with that of the water pentamers around TU. For the lowest-energy water pentamer in vacuum (the nonplanar nonsymmetric "uudud" structure[62]), we obtained an average O−O distance of 2.704 Å at the B3LYP/6-31G(d,p) level, whereas in the two water pentamers around TU, the average O−O distances are 2.812 and 2.858 Å.

From $TU-(H_2O)_6$ to $TU-(H_2O)_{16}$, one of the two hydrogen atoms of the NH_2 groups is involved in a stable hydrogen bond with water molecules with bond lengths of 1.96, 1.86, 1.95, and 1.95 Å, respectively (Figure 8f to i). However, for the same sequence, the hydrogen-bond length between the lower water molecules and the sulfur atom increases as the water cage around TU begins to form, indicating the prevalence of interwater hydrogen bonding. For $TU-(H_2O)_{16}$, these hydrogen bonds have lengths of 2.41 and 2.66 Å.

Table 11 contains electronic energies and interaction energies with the water molecules. Interaction energies were computed as the energy difference between the TU−water complex and the energies of the isolated TU and the water cluster with the same geometry as that in the TU−water complex. Interaction energies were corrected for the basis set superposition error (BSSE) using the counterpoise method of Boys and Bernardi.[63] All of the structures in Figure 8 were optimized at the B3LYP/6-31+G(d,p) level. Using these geometries, interaction energies with and without BSSE corrections were also computed with the 6-31+G(2d,2p) basis, as indicated in the last two columns of Table 11. The data in Table 11 show that the BSSE is small when taking into account the large size of the TU−water complexes. For example, for $TU-(H_2O)_{16}$, the BSSE is 3.8 kcal/mol at the 6-31+G(d,p) level and is only 2.1 kcal/mol with the more complete 6-31+G(2d,2p) basis. From now on, we will refer to only ΔE_{BSSE} calculated at the B3LYP/6-31+G(2d,2p) level in our discussion of the energetics of TU−water complexes.

The interaction of TU with a single water molecule is stronger when the latter hydrogen bonds to both the NH_2 group and the sulfur atom (Figure 8b, −9.4 kcal/mol) than when it binds to both NH_2 groups (Figure 8a, −6.5 kcal/mol). When two water molecules hydrogen bond to the NH_2 group and the S atom (Figure 8d), the interaction energy is much larger than when they hydrogen bond on top of the NH_2 groups (Figure 8c), −18.6 and −8.4 kcal/mol, respectively. Most of the interaction energy between TU and the water molecules is reached for the $TU-(H_2O)_6$ complex (Figure 8f). As shown in Figure 9, the addition of 10 more water molecules increases the interaction energy by only 3.8 kcal/mol. Figure 9 shows that the interaction energy of TU with water monotonically decreases up to a value of around −37 kcal/mol with a pronounced break in the plot for $n = 6$.

The consideration of the solvent changes the picture of TU adsorption on the metal. The microsolvation structures in Figure 8e−i show that the NH_2 groups get surrounded by the water cage with one of the hydrogen atoms of the NH_2 group forming a hydrogen bond with a water molecule. However, the structure of water around the sulfur atom is more open (Figure 8i), leaving this atom free to interact with the metal surface. We added four more water molecules to the $TU-(H_2O)_{16}$ structure on the sulfur side, but the additional water molecules formed new hydrogen bonds with the other waters instead of with the sulfur atom. Thus, the sulfur atom of TU is free to interact directly with the metal surface without any reorganization of the hydration shell. Adsorption of TU via the NH_2 groups (Figures 3b and 4) would first require the rupture of part of the hydration shell with the corresponding energy cost. Besides, these adsorption geometries require the removal of several water molecules from the surface. Therefore, adsorption via the sulfur atom seems to be the preferred geometry in solution. However, one may argue that the energy gain for adsorption via the sulfur atom (−12 kcal/mol on the hollow site) is compensated by the energy required to remove one or two water molecules from the electrode surface. In refs 58 and 64, we obtained a value of −8 kcal/mol for the binding energy of water on an on-top site of Ag(111). But it must also be considered that in a electrochemical environment the electric field of the interface greatly increases the binding energy of TU as we show in Figure 6a. Therefore, we conclude that on a positively charged surface (with an electric field pointing in the same direction as the dipole moment of TU) the preferred adsorption geometry of hydrated TU will have the molecular plane perpendicular to the surface with the sulfur atom bound to the metal.

On the Mechanism of Thiourea−Thioureate Conversion. Several conclusions may be drawn from the results of previous sections concerning the nature of the adsorbed species: (1) of all of the species considered, the strongest bonding to the surface occurs for the canonical TU radical suggesting that this should be most stable adsorbate; (2) the surface bonding of this radical has no major differences with that of the methanethiol radical supporting the XPS experimental evidence in this direction;[31] and (3) the enlargement of the SC bond upon adsorption for molecular TU is negligible, whereas for the canonical TU radical, this bond considerably increases, indicating a weakening of the bond strength compatible with the SC frequency downshift observed experimentally.[17−30] Therefore, the general conclusion is that TU interconverts upon adsorption into a canonical TU radical that bears a negative charge, giving rise to a thioureate anion, which has the same surface bonding as that of alkanethiols.

The next step was to try to understand the surface mechanism of TU−canonical TU radical interconversion. In this section, we first investigate this reaction in vacuum, and then we consider a model system that simulates the main features of the electrochemical interface.

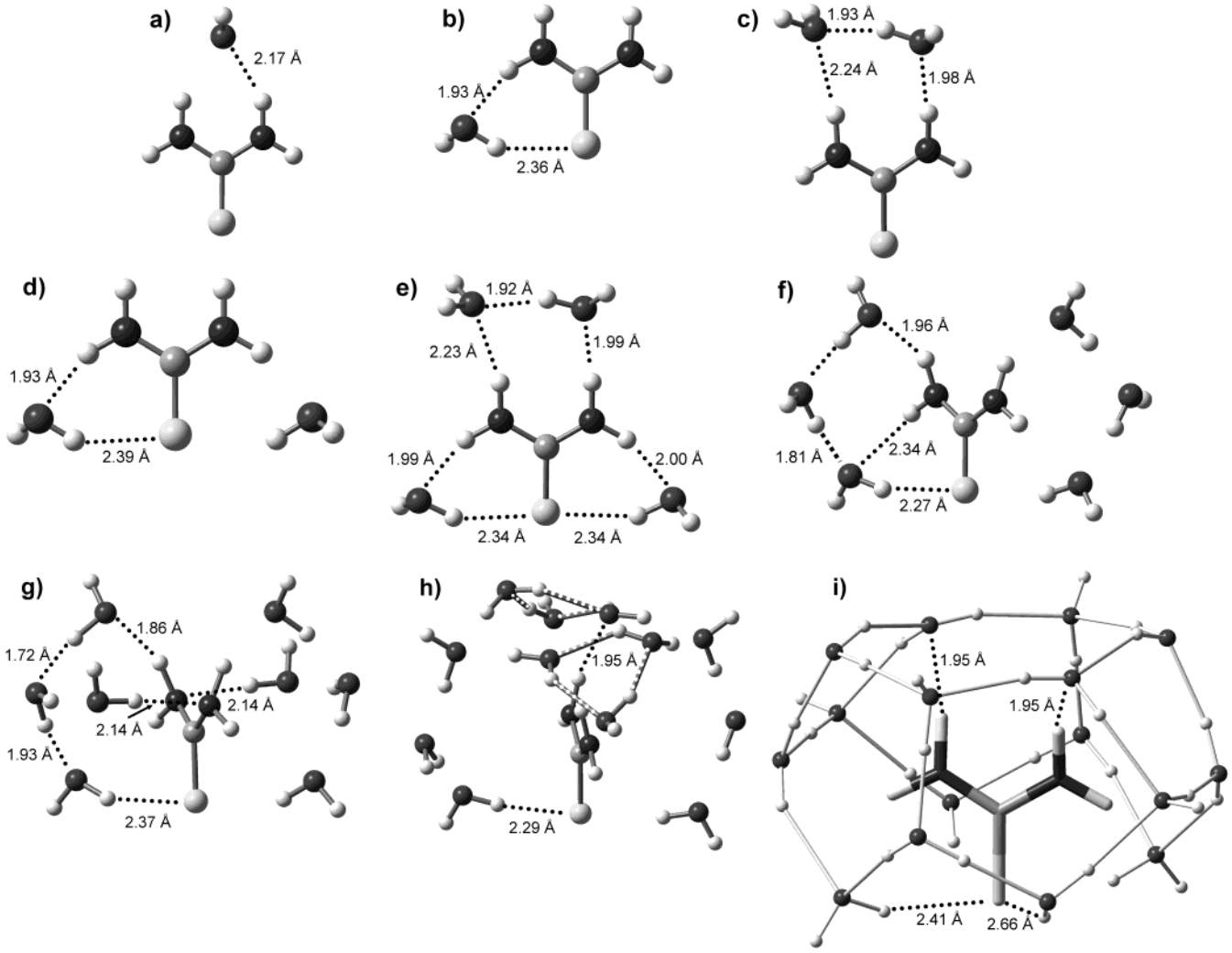

Figure 8. Equilibrium structures of thiourea hydrated with (a)and (b) 1, (c) and (d) 2, (e) 4, (f) 6, (g) 8, (h) 12, and (i) 16 water molecules. Note the formation of water tetramers and pentamers around thiourea in i. All structures correspond to true minima according to frequency analysis performed at the B3LYP/6-31+G(d,p) level.

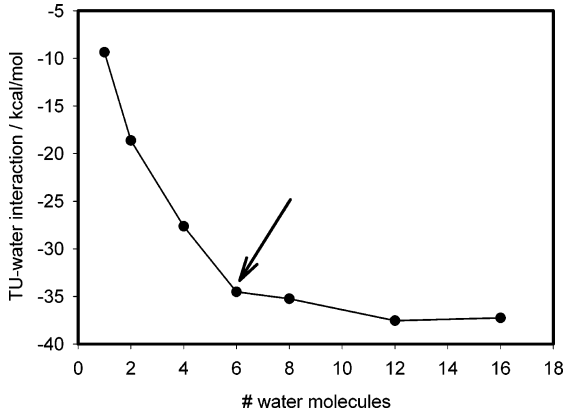

Figure 9. Thiourea−water interaction as a function of the number of water molecules. The arrow shows that most of the interaction is obtained with the first six water molecules. Geometries were optimized at the B3LYP/6-31+G(d,p) level, and final energies were calculated at the B3LYP/6-31+G(2d,2p) level with BSSE correction.

Surface Reaction in Vacuum. With the surface binding energies calculated in the previous sections, we can now evaluate the energy change ΔE for the surface reaction

$$SC(NH_2)_{2\,(surf)} \rightarrow SC(NH_2)(NH)_{\,(surf)} + H_{\,(surf)} \qquad (13)$$

TABLE 11: Interaction Energy of Thiourea with the Hydration Shell as a Function of the Number of Water Molecules[a]

	6-31+G(d,p)		6-31+G(2d,2p)	
n	ΔE	ΔE_{BSSE}	ΔE	ΔE_{BSSE}
1 (Figure 8a)	−8.4	−7.3	−7.0	−6.5
1 (Figure 8b)	−10.3	−9.6	−9.7	−9.4
2 (Figure 8c)	−10.4	−9.1	−8.9	−8.4
2 (Figure 8d)	−20.8	−19.3	−19.4	−18.6
4 (Figure 8e)	−31.9	−29.2	−28.9	−27.6
6 (Figure 8f)	−38.5	−36.3	−35.6	−34.5
8 (Figure 8g)	−40.4	−36.9	−37.0	−35.2
12 (Figure 8h)	−41.4	−38.9	−39.0	−37.5
16 (Figure 8i)	−41.9	−38.1	−39.4	−37.3

[a] Energies are in kcal/mol, TU−water complexes are optimized at the B3LYP/6-31+G(d,p) level, and the final energy is computed at the B3LYP/6-31+G(2d,2p) level.

in which an adsorbed TU molecule decomposes into a canonical TU radical and a hydrogen atom. ΔE is given by

$$\Delta E = -BE_{TU} + \Delta E_c + D_{SH} + BE_{rad} + BE_H \qquad (14)$$

as can be deduced from the following thermodynamic cycle: (a) TU desorption ($-BE_{TU}$), (b) TU conversion to canonical TU (ΔE_c), (c) canonical TU dissociation into a canonical TU

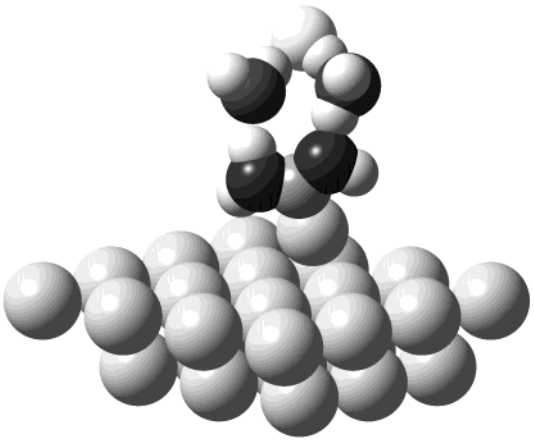

Figure 10. Oxidative adsorption of thiourea. Formation of canonical thiourea on a positively charged surface in the presence of a fluoride counterion. PW91/STO calculation performed with ADF.[45]

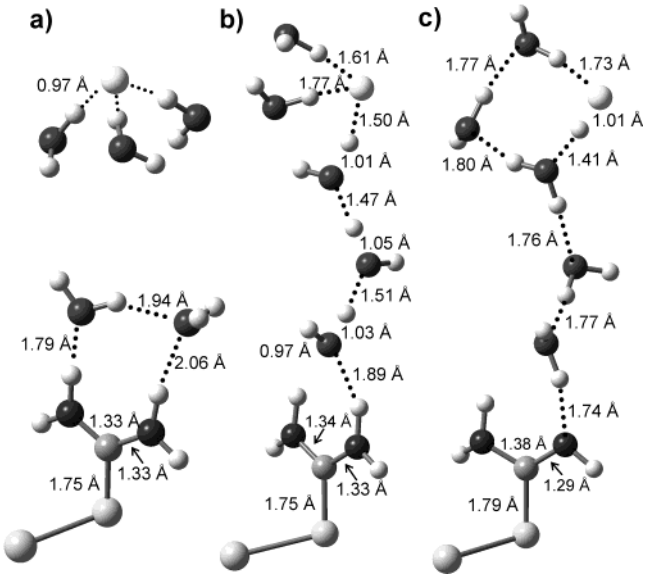

Figure 11. Reaction of a bihydrated TU molecule bound to an Ag^+ ion with a trihydrated fluoride ion. (a) Initial structure, (b) transition state, and (c) final structure. Optimization was performed by constraining the distance between the carbon atom of TU and the fluoride ion to 10 Å. B3LYP/6-31+G(d,p) calculation.

radical and a hydrogen atom (D_{SH}, the S−H bond energy), and (d) adsorption of the radical and the hydrogen atom ($BE_{rad} + BE_H$). ΔE_c and D_{SH} were calculated at the B3LYP/6-311+G-(2df,2p) level including ZPE corrections. We obtained $\Delta E_c = 11.9$ kcal/mol and $D_{SH} = 79.8$ kcal/mol. The S−H bond energy of canonical TU is very close to the value of 81.7 kcal/mol of cysteine and 81.9 of $HSCH_3$ reported in the literature at the B3LYP level.[65] The binding energy of H on Ag(111) was calculated with the ADF program on the same metal cluster that was used to calculate the binding energy of the canonical TU radical. The hcp hollow site is slightly more stable than the fcc site, giving a binding energy of $BE_H = -45.7$ kcal/mol. Sellers[57] obtained a binding energy of −56 kcal/mol at the MP2 level using a metal cluster to model the Ag(111). Our value is close to the experimental value of 52 kcal/mol.[66] Using $BE_{TU} = -33.2$ kcal/mol (Table 5, flat adsorption) and $BE_{rad} = -42.2$ kcal/mol (Table 6), we obtained $\Delta E = +37.0$ kcal/mol. Therefore, the reaction is very endothermic, and to proceed it will require some coupled chemical reactions. For example, the surface dissociation of $HSCH_3$ on gold to give $SCH_3 + H$ requires +11.3 kcal/mol.[57] But if the reaction between adsorbed hydrogen atoms to give adsorbed H_2 is considered, the energy change for the overall reaction $HSCH_3 \rightarrow SCH_3 + {}^1/_2H_2$ now decreases to +2.7 kcal/mol.[57]

Oxidative Adsorption under Electrochemical Conditions. In a previous section, we used homogeneous external electric fields as a first-order approximation to molecular adsorption in the electrochemical double layer. One advantage of this approach is that it allowed us to evaluate the contribution of the adsorbate polarization to the binding energy, which is important in the case of a molecule such as TU with a high dipole moment of 5.0 D. However, for a more complete description of the electrochemical interface, the model must describe several features such as charge transfer, an inhomogeneous electric field due to the presence of a counterion, and explicit consideration of some solvent molecules. This is a demanding task for ab initio calculations because an adequate description of the metal surface requires a large metal cluster and an adequate description of the solvent requires us to consider many water molecules.

The different features of the electrochemical interface were introduced step by step to model the oxidative adsorption of TU. The steps considered were (a) adsorption of molecular TU on a metal cluster with a positive charge of +1 as a model of a positively charged surface; (b) addition of water molecules on top of TU; and (c) addition of a fluoride ion as a prototype counterion to ensure electroneutrality of the whole system. This in turn produces an inhomogeneous electric field around the adsorbate. The surface charge of the positively charged cluster (the 25-atom cluster shown in Figure 10) was estimated by comparing its Mulliken populations with those of the uncharged cluster. An average surface charge of 0.17 $\mu C/cm^2$ was obtained. In the usual practice of making a self-assembled monolayer, one dips a substrate piece into the solution containing a thiol without potential control. In the case of silver, the open-circuit potential during the formation of a monolayer is considerably more positive[67] than the potential of zero charge (−0.932 V in NaF[68]), indicating that the metal surface is positively charged. This is the reason that we considered a positive surface to be the starting point of our modeling.

The adsorption of molecular TU on the positively charged surface is 9 kcal/mol more stable than that on the neutral surface, and the sulfur distance above the surface decreases to 2.61 Å from the value of 2.80 Å corresponding to the uncharged surface. In turn, the SC bond length increases to 1.717 Å from the vacuum value of 1.668 Å. The increase in bond length results from a charge transfer of 0.3 electrons from TU to the surface, which produces a depletion of electron density along the SC bond. At this stage, the N−H bond length does not appreciably change. However, when two water molecules are added on top of TU (with the starting geometry of Figure 8c) together with a fluoride anion and the geometry of the system is optimized, one of the NH_2 groups loses a hydrogen atom, and hydrogen fluoride is produced. The final structure is given in Figure 10, which shows that the interconversion of TU into canonical TU readily occurs on the positively charged surface.

The electrolyte modeling in Figure 10 is rather limited mainly because the hydration shell of fluoride has not been taken into account. One point to consider is that the diameter of a small hydrated ion such as fluoride is around 10 Å, thus it will not be as close to the TU molecule as shown in Figure 10, with the corresponding influence on the electric field around TU. Therefore, to improve the description of the electrolyte and to obtain deeper insight into the mechanism of proton transport, we considered a model system in which a bihydrated TU molecule bound to a single Ag^+ ion reacts with a trihydrated

fluoride ion (Figure 11a). The initial geometry shown in Figure 11a was built by first optimizing a bihydrated TU molecule on an Ag^+ ion to model the adsorption on the positively charged metal. Then the counterion (trihydrated fluoride) was added to ensure electroneutrality. The geometry of the initial system (Figure 11a) was optimized, keeping the distance between the carbon atom of TU and the fluorine atom at 10 Å. Figure 11b and c shows the transition state (TS) as well as the final structure for this reaction. A chain of water molecules is formed between TU and the fluoride ion. In the TS, the OH bond lengths of the water molecules along the chain direction are increased with an average value of 1.037 Å, whereas the other OH bond lengths of the water molecules are 0.969 Å. Figure 11b also shows that the hydrogen-bond lengths between the water molecules are very short, with an average value of 1.494 Å. The SC bond length in the TS increases to 1.753 Å from the vacuum value of 1.674 (B3LYP/6-31+G(d,p). This value is comparable to the value of 1.717 Å of molecular TU adsorbed on the charged surface (Figure 10), indicating that the simplified representation of the surface in Figure 11 is still adequate. The N−H bonds in the TS are only slightly lengthened with respect to the vacuum values (1.034 vs 1.011 Å).

The reaction path from the TS (Figure 11b) to the final structure (Figure 11c) is characterized by the simultaneous lengthening of the N−H bond of TU and the O−H bonds of the water molecules along the water-chain direction. In this way, the proton transfer occurs in a concerted manner until canonical TU and hydrogen fluoride are generated in the final state. As the proton transfer proceeds, charge transfer toward the silver atom occurs. The effective charges of the silver atom for the reactants, transition state, and products (Figure 11) are +0.3, +0.26, and +0.15, respectively, indicating that from the initial to the final state 0.15 electron is transferred to the silver atom, which thus becomes less positively charged. These results support investigations that indicate that electrochemical electron-transfer steps are involved in the adsorption of alkanethiols.[67] In summary, the main features of the oxidative adsorption of TU on a positively charged surface are (a) on the electrolyte side, the rupture of the N−H bond and proton-transfer reaction into the solution and (b) on the metal side, the weakening of the S−C bond and the formation of the S−Ag bond accompanied by charge transfer toward the metal.

To understand the mechanism of oxidative adsorption in very alkaline or acidic solutions, we need to consider that in the extreme pHs the predominant species are thioureate and thiouronium ions. For the adsorption of a thioureate anion, we can predict that the charge transfer toward the surface will be ca. 0.8 electron because the final charge of the adsorbate is 0.2 electron (Table 6). Although the data in Table 6 corresponds to the adsorption of the radical and not the anion, we know from our previous work on ionic adsorption that the state of an adsorbate is the same whether it is adsorbed from the neutral particle, the cation, or the anion.[69,70] However, the mechanism of oxidative adsorption of the thiouronium cation requires further investigations because the release of two protons is required to produce adsorbed thioureate.

Conclusions

Quantum mechanical calculations at different levels of theory were employed to investigate the adsorption of different thiourea species on Ag(111). Electric field and solvent effects were considered with the objectives of (a) elucidating the nature of the adsorbed species, mainly in an electrochemical environment and (b) understanding the energetics and mechanisms of the surface reactions, particularly the oxidative adsorption of thiourea.

We first investigated the adsorption of thiourea, canonical thiourea, and formamidine disulfide at the Ag(111)/vacuum interface. The most stable adsorption geometry for thiourea corresponds to a flat configuration with a binding energy of −33.2 kcal/mol. However, upright adsorption via the sulfur atom has the lowest binding energy (−12 kcal/mol). The adsorbate relaxation induced by the adsorption process is very small. For example, the SC bond length increases by only 0.02 Å. The binding energies of molecular canonical thiourea, $(NH)(NH_2)$-CSH, are comparable to those of thiourea on equivalent surface sites. However, the surface reaction for thiourea → canonical thiourea interconversion is endothermic by 15.7 kcal/mol; as a consequence, canonical TU is 11.4 kcal/mol higher in energy than thiourea. Formamidine disulfide adsorbs on Ag(111) with a binding energy of 17.0 kcal/mol, but the adsorption is dissociative, generating two canonical thiourea radicals, $(NH)(NH_2)CS^{\bullet}$, in an exothermic reaction with $\Delta E = -17.4$ kcal/mol. Therefore, of all of the molecular species considered, thiourea is the only stable species at the Ag(111)/vacuum interface.

The adsorption of the canonical thiourea radical, $(NH)(NH_2)$-$CS^{\bullet}$, has a binding energy of −42.2 kcal/mol on the fcc hollow site. The surface bonding of this radical shows no major differences with that of the methanethiol radical when parameters such as binding energy, adsorbate charge, and adsorbate−surface distance are considered. The surface bonding produces an important relaxation of canonical TU. In particular, the SC bond length increases ca. 0.2 Å with the corresponding implications in the vibrational modes in which this bond participates.

To understand the nature of the surface reactions in which thiourea is involved at the electrochemical interphase, we investigated electric field and solvent effects. Externally applied positive electric fields, which induce a positive charge on the metal surface, greatly strengthen the surface bond, inducing an upright adsorption geometry via the sulfur atom. The increased binding energy has contributions from the polarization of the molecule as well as from a strengthened sulfur−surface bond as a consequence of the electrostatic interaction of the negatively charged sulfur atom and the positively charged surface.

Solvent effects were first considered for thiourea in solution to determine the nature of the predominant species in acidic and basic electrolytes. The reactions with hydroxide and hydronium ions in which thioureate and thiouronium ions are produced have free-energy changes of +3.6 and −4.9 kcal/mol, respectively. Therefore, the thiouronium ion is the predominant species in solution, whereas in neutral and alkaline solutions, thiourea predominates. The interconversion of thiourea into canonical thiourea in solution has $\Delta G_{298} = 16.1$ kcal/mol, whereas the value in vacuum is $\Delta G_{298} = 11.4$ kcal/mol, indicating that canonical thiourea is destabilized by the solvent.

The study of the microsolvation of thiourea showed that water molecules form a compact cage around thiourea that consists of linked water tetramers and pentamers. Only one of the hydrogen atoms of the NH_2 group of thiourea forms a hydrogen bond with water with a bond length of 1.95 Å ($TU-(H_2O)_{16}$ structure). The interaction energy of TU with water rapidly stabilizes to a value of −34.5 kcal/mol after the first 6 water molecules are added and increases to only −37.3 kcal/mol when 16 water molecules are around TU. The sulfur atom of TU is poorly hydrated, indicating that surface adsorption via this atom

will be energetically favored because it will not affect the structure of the solvent around TU. Therefore, a consideration of both electric field and solvent effects points toward an upward adsorption of TU via the sulfur atom in solution.

The surface bond strength of the canonical thiourea radical led us to investigate the mechanisms by which this radical is generated on the surface from the thiourea molecule. At the Ag(111)/vacuum interface, the surface reaction $(NH_2)_2CS \rightarrow (NH)(NH_2)CS + H$ is very endothermic, with $\Delta E = 37$ kcal/mol. Thus, thiourea radical formation seems unlikely in vacuum unless there are coupled chemical reactions that could lower the energy change of the net surface reaction.

Next, we considered the electrochemical reaction of the oxidative adsorption of thiourea. The reaction was modeled on a positively charged surface because this will be the most likely situation for silver under open-circuit conditions. The solvent was considered explicitly including some water molecules and a fluoride anion to ensure the electroneutrality of the whole system. The transition state for this reaction is characterized by the formation of a chain of water molecules (with short hydrogen bonds) between thiourea and the fluoride ion. The reaction path towards the products shows that the proton transfer from thiourea toward the fluoride anion occurs by the simultaneous lengthening of one of the N−H bonds of TU and the O−H bonds of the water molecules. Simultaneously, a charge-transfer process is observed from thiourea toward the metal. In the final state, a canonical thiourea radical is formed with an enlarged SC bond as compared to that of thiourea. These results support the proposed mechanism of the adsorption of alkanethiols consisting of an electrochemical reaction.[67]

Acknowledgment. E.M.P. thanks Fundación Antorchas for grant A-13532/1-102. P.P.-O. thanks CONICET for a PEI grant. We also are grateful for the support of Agencia Nacional de Promoción Científica y Tecnológica (grant no. 06-03195), Agencia Córdoba Ciencia and SECYT-UNC. F.P.C. thanks Agencia Córdoba Ciencia and CONICET for the fellowships granted.

References and Notes

(1) Mendez, S.; Andreasen, G.; Schilardi, P.; Figueroa, M.; Vázquez, L.; Salvarezza, R. C.; Arvia, A. J. *Langmuir* **1998**, *14*, 2515.

(2) Azzaroni, O.; Schilardi, P. L.; Salvarezza, R. C.; Arvia, A. J. *Langmuir* **1999**, *15*, 1508.

(3) Kozlov, V. M.; Peraldo Bicelli, L. *Mater. Chem. Phys.* **2000**, *62*, 158.

(4) Wünsche, M.; Meyer, H.; Schumacher, R. *Electrochim. Acta* **1995**, *40*, 629.

(5) Upadhyay, D. N.; Yegnaraman, V. *Mater. Chem. Phys.* **2000**, *62*, 247.

(6) Yazici, B.; Arslan, G.; Erbil, M.; Zor, S. *Int. J. Hydrogen Energy* **1998**, *23*, 867.

(7) Yan, M.; Liu, K.; Jiang, Z. *J. Electroanal. Chem.* **1996**, *408*, 225.

(8) Bolzán, A. E.; Wakenge, I. B.; Salvarezza, R. C.; Arvia, A. J. *J. Electroanal. Chem.* **1999**, *475*, 181.

(9) Stankovic, Z. D.; Vikovic, M. *Electrochim. Acta* **1996**, *41*, 2529.

(10) Cheng, X. L.; Ma, H. Y.; Chen, S. H.; Yu, R.; Chen, X.; Yao, Z. M. *Corrosion Sci.* **1999**, *41*, 321.

(11) Bolzán, A. E.; Haseeb, A. S. M. A.; Schilardi, P. L.; Piatti, R. C. V.; Salvarezza, R. C.; Arvia, A. J. *J. Electroanal. Chem.* **2001**, *500*, 533.

(12) Bolzán, A. E.; Wakenge, I. B.; Piatti, R. C. V.; Salvarezza, R. C.; Arvia, A. J. *J. Electroanal. Chem.* **2001**, *501*, 241.

(13) Gassa, L. M.; Lambi, J. N.; Bolzán, A. E.; Arvia, A. J. *J. Electroanal. Chem.* **2002**, *527*, 71.

(14) Szklarczyk, M.; Smolinski, S. *J. Electroanal. Chem.* **1995**, *390*, 109.

(15) Szklarczyk, M.; Hoa, N. N.; Zelenay, P. *J. Electroanal. Chem.* **1996**, *405*, 111.

(16) Lukomska, A.; Smolinski, S.; Sobkowski, J. *Electrochim Acta* **2001**, *46*, 3111.

(17) Fleischmann, M.; Hill, I. R.; Sundholm, G. *J. Electroanal. Chem.* **1983**, *157*, 359.

(18) Hajbi, A.; Chartier, P.; Goetz-Grandmont, G.; Leroy, M. *J. Electroanal. Chem.* **1987**, *227*, 159.

(19) Tian, Z. Q.; Lian, Y. Z.; Fleischmann, M. *Electrochim. Acta* **1990**, *35*, 879.

(20) Kim, H.; Kim, J. J. *J. Raman Spectrosc.* **1993**, *24*, 77.

(21) Tian, Z. Q.; Li, W. H.; Mao, B. W.; Gao, J. S. *J. Electroanal. Chem.* **1994**, *379*, 271.

(22) Bukowska, J.; Jackowska, K. *J. Electroanal. Chem.* **1994**, *367*, 41.

(23) Loo, B. H. *Chem. Phys. Lett.* **1982**, *8*, 346.

(24) Loo, B. H.; Leahey, J.; Lee, Y. G. *Chem. Phys. Lett.* **1990**, *172*, 33.

(25) Loo, B. H.; Lee, Y. G.; Kato, T. *Bull. Chem. Soc. Jpn.* **1991**, *64*, 3126.

(26) Brown, G. M. *J. Electroanal. Chem.* **1995**, *380*, 161.

(27) Brown; G. M.; Hope, G. A. *J. Electroanal. Chem.* **1996**, *413*, 153.

(28) Joy, V. T.; Srinivasan, T. K. K. *Spectrochim. Acta A* **1999**, *55*, 2899.

(29) Reents, B.; Plieth, W.; Macagno, V. A.; Lacconi, G. I. *J. Electroanal. Chem.* **1998**, *453*, 121.

(30) Yao, J. L.; Mao, B. W.; Gu, R. A.; Tian, Z. Q. *Chem. Phys. Lett.* **1999**, *306*, 314.

(31) Brunetti, V.; Blum, B.; Salvarezza, R. C.; Arvia, A. J.; Schilardi, P. L.; Cuesta, A.; Gayone, J. E.; Zampieri, G. *J. Phys. Chem. B* **2002**, *106*, 9831.

(32) Brunetti, V.; Blum, B.; Salvarezza, R. C.; Arvia, A. J. *Langmuir* **2003**, *19*, 5336.

(33) Olah, G. A.; Burrichter, A.; Rasul, G.; Christe, K. O.; Surya Prakash, G. K. *J. Am. Chem. Soc.* **1997**, *119*, 4345.

(34) Masunov, A.; Dannenberg, J. J. *J. Phys. Chem. B* **2000**, *104*, 806

(35) Bencivenni, L.; Nunziante Cesaro, S.; Pieretti, A. *Vib. Spectrosc.* **1998**, *18*, 91.

(36) (a) Mamann, D. R. *Phys. Rev. B* **1997**, R10157. (b) Maerker, C.; Schleyer, P. V. R.; Liedl, K. R.; Ma, T.-K.; Quack, M.; Suhn, M. A. *J. Comput. Chem.* **1997**, *18*, 1695. (c) Kim, K.; Jordan, K. D. *J. Phys. Chem.* **1994**, *98*, 10089. (d) Lee, H. M.; Suh, S. B.; Lee, J. Y.; Tarakeshwar, P.; Kima, K. S. *J. Chem. Phys.* **2000**, *112*, 9759. (e) Hamad, S.; Lago, S.; Mejías, J. A.; *J. Phys. Chem. A* **2002**, *106*, 9104. (f) Lee, J. Y.; Kim, J.; Lee, H. M.; Tarakeshwar, P.; Kim; K. S. *J. Chem. Phys.* **2000**, *113*, 6160.

(37) Frisch, M. J.; Trucks, G. W.; Schlegel, H. B.; Scuseria, G. E.; Robb, M. A.; Cheeseman, J. R.; Montgomery, J. A., Jr.; Vreven, T.; Kudin, K. N.; Burant, J. C.; Millam, J. M.; Iyengar, S. S.; Tomasi, J.; Barone, V.; Mennucci, B.; Cossi, M.; Scalmani, G.; Rega, N.; Petersson, G. A.; Nakatsuji, H.; Hada, M.; Ehara, M.; Toyota, K.; Fukuda, R.; Hasegawa, J.; Ishida, M.; Nakajima, T.; Honda, Y.; Kitao, O.; Nakai, H.; Klene, M.; Li, X.; Knox, J. E.; Hratchian, H. P.; Cross, J. B.; Adamo, C.; Jaramillo, J.; Gomperts, R.; Stratmann, R. E.; Yazyev, O.; Austin, A. J.; Cammi, R.; Pomelli, C.; Ochterski, J. W.; Ayala, P. Y.; Morokuma, K.; Voth, G. A.; Salvador, P.; Dannenberg, J. J.; Zakrzewski, V. G.; Dapprich, S.; Daniels, A. D.; Strain, M. C.; Farkas, O.; Malick, D. K.; Rabuck, A. D.; Raghavachari, K.; Foresman, J. B.; Ortiz, J. V.; Cui, Q.; Baboul, A. G.; Clifford, S.; Cioslowski, J.; Stefanov, B. B.; Liu, G.; Liashenko, A.; Piskorz, P.; Komaromi, I.; Martin, R. L.; Fox, D. J.; Keith, T.; Al-Laham, M. A.; Peng, C. Y.; Nanayakkara, A.; Challacombe, M.; Gill, P. M. W.; Johnson, B.; Chen, W.; Wong, M. W.; Gonzalez, C.; Pople, J. A. *Gaussian 03*, revision B.04; Gaussian, Inc.: Pittsburgh, PA, 2003.

(38) Kristyán, S.; Pulay, P. *Chem. Phys. Lett.* **1994**, *229*, 175.

(39) Huzinaga, S.; Klubokowski, M.; Sakai, Y. *J. Phys. Chem.* **1984**, *88*, 4880.

(40) Andzelm, J.; Huzinaga, S.; Klubokowski, M.; Radzio, E. *Mol. Phys.* **1984**, *52*, 1495.

(41) Huzinaga, S.; Seijo, L.; Barandiaran, Z.; Klubokowski, M. *J. Chem. Phys.* **1987**, *86*, 2132.

(42) Dunning, T. H. *J. Chem. Phys.* **1970**, *53*, 2823.

(43) *CRC Handbook of Chemistry and Physics*, 62nd ed.; Weast, R. C. Ed.; Chemical Rubber Company: Boca Raton, FL, 1982.

(44) Patrito, E. M.; Paredes-Olivera, P.; Sellers, H. *J. Mol. Struct.: THEOCHEM* **1996**, *388*, 209.

(45) Baerends, E. J.; Bérces, A.; Bo, C.; Boerrigter, P. M.; Cavallo, L.; Deng, L.; Dickson, R. M.; Ellis, D. E.; Fan, L.; Fischer, T. H.; Fonseca Guerra, C.; van Gisbergen, S. J. A.; Groeneveld, J. A.; Gritsenko, O. V.; Harris, F. E.; van den Hoek, P.; Jacobsen, H.; van Kessel, G.; Kootstra, F.; van Lenthe, E.; Osinga, V. P.; Philipsen, P. H. T.; Post, D.; Pye, C. C.; Ravenek, W.; Ros, P.; Schipper, P. R. T.; Schreckenbach, G.; Snijders, J. G.; Sola, M.; Swerhone, D.; te Velde, G.; Vernooijs, P.; Versluis, L.; Visser, O.; van Wezenbeek, E.; Wiesenekker, G.; Wolff, S. K.; Woo, T. K.; Ziegler, T.; Fonseca Guerra, C.; Snijders, J. G.; te Velde, G.; Baerends, E. J. *Theor. Chem. Acc.* **1998**, *99*, 391.

(46) Vosko, S. H.; Wilk, L.; Nusair, M. *Can. J. Phys.* **1980**, *58*, 1200.

(47) Becke, A. D. *Phys. Rev. A* **1988**, *38*, 3098.

(48) Perdew, J. P.; Wang, Y. *Phys. Rev. B* **1992**, *45*, 13244.

(49) Lee, C.; Yang, W.; Parr, R. G. *Phys. Rev. B* **1988**, *37*, 785.

(50) Perdew, J. P.; Burke, K.; Wang, Y. *Phys. Rev. B* **1996**, *54*, 16533.
(51) van Lenthe, E.; Ehlers, A. E.; Baerends, E. J. *J. Chem. Phys.* **1999**, *110*, 8943.
(52) Sellers, H.; Ulman, A.; Shnidman, Y.; Eilers, J. E. *J. Am. Chem. Soc.* **1993**, *115*, 9389.
(53) Ferral, A.; Paredes-Olivera, P.; Macagno, V. A.; Patrito, E. M. *Surf. Sci.* **2003**, *525*, 85.
(54) Cossi, M.; Scalmani, G.; Raga, N.; Barone, V. *J. Chem. Phys.* **2002**, *117*, 43.
(55) Shustorovich, E.; Sellers, H. *Surf. Sci. Rep.* **1998**, *31*, 1.
(56) Vargas, M. C.; Giannozzi, P.; Selloni, A.; Scoles, G. *J. Phys. Chem. B* **2001**, *105*, 9509.
(57) Sellers, H. *Surf. Sci.* **1993**, *294*, 99.
(58) Paredes-Olivera, P.; Ferral, A.; Patrito, E. M. *J. Phys. Chem. B* **2001**, *105*, 7227.
(59) Bogus, P. S.; Puccini, G.; Philpot, M. R. *J. Chem. Phys.* **1989**, *90*, 4287.
(60) McQuarrie, D. A. *Statistical Mechanics*; Harper and Row: New York, 1976.
(61) Csajka, F. S.; Chandler, D. *J. Chem. Phys.* **1998**, *109*, 1125.
(62) Graf, S.; Mohr, W.; Leutwyler, S. *J. Chem. Phys.* **1999**, *110*, 7893.
(63) (a) Boys, S. F.; Bernardi, F. *Mol. Phys.* **1970**, *19*, 553. (b) Simon, S.; Duran, M.; Dannenberg, J. J. *J. Chem. Phys.* **1996**, *105*, 11024.
(64) Patrito, E. M.; Paredes-Olivera, P. *Surf. Sci.* **2003**, *527*, 149.
(65) Himo, F.; Eriksson, L. A. *J. Am. Chem. Soc.* **1998**, *120*, 11449.
(66) Shustorovich, E. *Adv. Catal.* **1990**, *37*, 101.
(67) Paik, W.-K.; Eu, S.; Lee, K.; Chon, S.; Kim, M. *Langmuir* **2000**, *16*, 10198.
(68) Shumilova, N. A.; Zhutaeva, G. V. In *Encyclopedia of Electrochemistry of the Elements*; Bard, A. J., Ed.; Marcel Dekker: New York, 1978; Chapter VIII-1, pp 66−67.
(69) Sellers, H.; Patrito, E. M.; Paredes-Olivera, P. *Surf. Sci*. **1996**, *352*, 222.
(70) Patrito, E. M.; Paredes-Olivera, P. *Electrochim. Acta* **1998**, *44*, 1237.